

Representing the ship magnetic field using prolate spheroidal harmonics –a comparative study of methods¹

S. A. Synnes⁺, P. A. Brodtkorb⁺ and E. S. A. M. Lepelaars^{*}

⁺Norwegian Defence Research Establishment (FFI), Kjeller and Horten, Norway

^{*}The Netherlands Organisation for Applied Scientific Research (TNO), The Hague, The Netherlands

Contact author email: Stig-Asle.Synnes@ffi.no

Abstract— The prolate spheroidal harmonics are well suited for describing the magnetic field of a vessel. In this article we discuss several strategies to improve the estimation of the model parameters based on measured field data. In particular we give an analytic expression for the maximum supported set of harmonics for any rectangular grid. This expression allows for automatic selection of the appropriate set of harmonics without the presently required amount of manual tuning. In addition, we demonstrate that normalization of the harmonics before the inversion is essential to get a robust estimate of the parameters.

I. INTRODUCTION

It is crucial to know the external magnetic field induced by marine vehicles in many practical applications [1]. Naval vessels and geophysical surveying ships, for example, have strict requirements for magnetic silencing. For these ships it is an absolute necessity to assess the external fields, since it determines the vessels vulnerability to detection and recognition.

A model of the source is required in order to evaluate the field at any external position, and several candidates have been investigated [1], [2]. We adopt the series expansion on prolate spheroidal harmonics. This model allows for representing both the near field and the far field by obtaining only a limited number of parameters.

The process of obtaining the appropriate set of expansion coefficients based on measured field data is solving the *inverse problem*. The quality of the estimated expansion coefficients is affected by positioning and orientation error. In addition to sensor and environmental noise, special care must be taken of aliasing problems due to a coarse sampling grid. Expanding the harmonics on the best centre point and focal distance is also crucial in order to terminate the series

expansion without introducing a major distortion. Furthermore, solving the inverse problem for the prolate spheroidal harmonics is sensitive to the set of harmonics included with each measurement grid. An ill-conditioned stated problem could lead to severe effects from series termination, sensor inaccuracies and noise. Some of these effects can be reduced following [3].

This article discusses several strategies to improve the inversion. In particular we give an analytic expression for the maximum supported set of basis functions for any rectangular grid. This expression allows for automatic selection of the appropriate set of harmonics without the presently required amount of manual tuning. In addition, we demonstrate that normalization of the harmonics before inversion is essential to get a robust estimate.

Limiting the set of harmonics to those supported by the measurement grid, normalizing and utilizing truncated singular value decomposition, contributes to a combined effect. The resulting series expansion describes the near field very accurately and without aliasing. Given sufficient information from near field measurements, even the far field can be accurately represented. A set of quality measures is suggested and used to validate the application of the method on real measurements. The findings using real measurement are in accordance with those of simulated sources.

The outline of the paper is as follows. Section II discusses the general setup and the forward problem. We propose a simple relationship between the set of coefficients that should be taken into account on one hand and the source length and the density of the measurement grid on the other hand in section III. Section IV introduces three quality measures that are employed to demonstrate this relationship using computer simulations. In Section V the results of these simulations are presented and discussed. Furthermore, the difference between using an exact and an approximate centre point and focal distance on the inversion procedure is illustrated. The gained

¹ Previously published at the MARELEC 2006 conference on maritime electromagnetism, Amsterdam, The Netherlands. Updates apply to sections III.B and III.D.2.

insight is applied in an inversion procedure on measured magnetic field data of a merchant ship in section VI. Section VII gives the conclusions.

II. PROLATE SPHEROIDAL HARMONIC SERIES EXPANSION

The prolate spheroidal coordinate system (ξ, η, φ) with focal length f is visualized in a Cartesian system (x, y, z) in Fig. 1. The conversion of coordinates given in [4] is adopted. In the following it is assumed, without loss of generality, that the prolate spheroidal coordinate system has the major axis along the centre-line of the vessel, in x -direction. The y -direction is pointing to the starboard side and the z -direction is pointing vertically down.

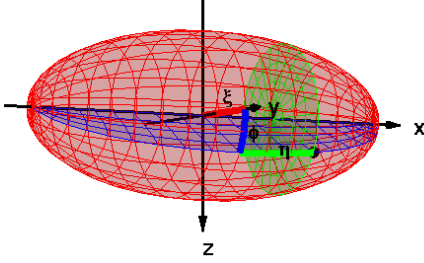


Fig. 1. Prolate spheroidal coordinates visualized in a Cartesian coordinate system

Solving Maxwell's equations for a source free region outside an isosurface boundary results in a magnetic field given by $\vec{H} = -\nabla\Phi$ and the magnetic flux density by $\vec{B} = \mu\vec{H}$, where μ is the magnetic permeability of the medium. In the source free region, the scalar potential Φ satisfies Laplace's equation $\nabla^2\Phi = 0$. In a prolate spheroidal coordinate system (ξ, η, φ) with focal length f , the scalar potential can be expanded as

$$\Phi = \sum_{n=0}^{\infty} \sum_{m=0}^n Q_n^m(\xi) P_n^m(\eta) [c_n^m \cos(m\varphi) + s_n^m \sin(m\varphi)] \quad (1)$$

where P_n^m and Q_n^m are the associated Legendre functions² of the first and second kind, respectively, of n -th degree and m -th order. The coefficients c_n^m and s_n^m are the expansion coefficients for each degree and order.

The prolate spheroidal harmonics are orthogonal on any isosurface ellipsoid, because the trigonometric functions and the associated Legendre functions of the first kind are both orthogonal. Thus the expansion coefficients can be determined from measurements on the ellipsoid alone. Correspondingly, measurements on a section of the ellipsoid should be sufficient to describe the field beyond this area. This will be elaborated

² The sign convention of omitting the Condon-Shortley phase is adopted. The associated Legendre functions of the second kind are evaluated following [5]

further in the following sections.

III. THE INVERSE PROBLEM

The expansion coefficients can be estimated by solving the inverse problem

$$\mathbf{F}\mathbf{a} = \mathbf{b}, \quad (2)$$

where the vector \mathbf{a} contains the unknown expansion coefficients to be determined. The vector \mathbf{b} contains the measured fields and the matrix \mathbf{F} contains the fields at the measurement points of the harmonics for unit coefficients.

Note that in Eq. (1) the coefficients s_n^0 are always multiplied by zero and the coefficient c_0^0 represents the field of a magnetic monopole [6], which does not exist. Thus these coefficients are excluded from the computations by arranging the unknown expansion coefficients as follows

$$\mathbf{a} = [c_1^0, c_1^1, s_1^1, c_2^0, c_2^1, s_2^1, c_2^2, s_2^2, \dots]^T.$$

The magnetic flux density related to each prolate spheroidal harmonic at each point of the grid are arranged column-wise to construct the matrix

$$\mathbf{F} = [\mathbf{f}_{c_1^0}, \mathbf{f}_{c_1^1}, \mathbf{f}_{s_1^1}, \mathbf{f}_{c_2^0}, \mathbf{f}_{c_2^1}, \mathbf{f}_{s_2^1}, \mathbf{f}_{c_2^2}, \mathbf{f}_{s_2^2}, \dots].$$

The least square solution to Eq. (2) is given by

$$\mathbf{a} = \mathbf{F}^\dagger \mathbf{b} \quad (3)$$

where \mathbf{F}^\dagger is the pseudoinverse of \mathbf{F} .

For a practical inversion scheme, only a limited set of harmonics can be computed, and the series expansion must be truncated. For valid estimation of expansion coefficients, the harmonics required to represent the field must be included, along with enough samples to discriminate between these harmonics. Because the lower degree harmonics decay more slowly than those of higher degree, a terminated series supports a good representation of the field beyond the measurement plane.

A series of considerations apply on selecting measurement grid, terminating the series expansion, etc. and are detailed in the forthcoming subsections.

A. Sampling criterion

Usually the measurement area is restricted to below the ship, and often the sensor grid is very coarse in the athwart ship direction. However, the source field must be sampled at a

sufficiently dense grid to represent the prominent features of the field at the measurement depth. If the measurements do not appear to be reasonably sampled (over-sampled) in either direction on the plane, more measurements must be added in order to represent the field with confidence.

B. Supported harmonics

In this subsection we derive an analytic expression for the maximum supported set of basis functions for any rectangular grid. This is essential in order to know which prolate spheroidal harmonics can be distinguished from measurements on a fixed sensor grid.

From Eq. (1), we find that the athwart ship resolution is related to the trigonometric function by its argument $m\varphi$, and the along ship resolution is mainly related to the associated Legendre functions of the first kind with degree n and order m .

The trigonometric functions are periodic, and in order to discriminate between functions up to periodicity m , a minimum of $2m$ samples of the scalar potential at different aspects (to the side of the ship) are required. By using the gradient of the scalar potential, as applied for 3-axis magnetic measurements, one ambiguity on the phase is avoided and only half the number of samples is required. For a measurement grid with N_y 3-axis magnetic sensors at different athwart ship positions, harmonics of order up to m_{\max} given by Eq. (4) can be distinguished.

$$m_{\max} = N_y \quad (4)$$

By inspection we find that the associated Legendre functions of the first kind are close to periodic in the along ship direction. The scalar potential oscillations over the coordinate span of η correspond to $(n-m+1-\delta_m)$ periods of the trigonometric functions. Here δ indicates the Kronecker delta. The same argumentation applied on the athwart ship resolution is now applied for a measurement grid with $N_{x,ship}$ samples taken within the ship length (for each of the N_y signatures recorded at different athwart ship positions). We obtain that harmonics of degree up to n_{\max} given by Eq. (5) can be distinguished using 3-axis measurements.

$$n_{\max}(m) \approx N_{x,ship} + m \quad (5)$$

For single axis measurements, ambiguities are introduced on the amplitude and phase of the scalar potential. Our experience suggests that for single axis measurements, twice the number of samples is required as compared with 3-axis measurements.

C. Choice of centre point and focal length

From the spherical harmonics we know that the series expansion of an off-centre located point source will introduce correctional terms corresponding to all sources of higher degree [7]. For the prolate spheroidal harmonics, similar relations apply, only that here the centre point, focal length and orientation of the main axis must all be considered.

With an unfortunate choice of the centre point or focal length, the inversion will depend on a long series of harmonics that is not necessarily supported by the grid. (As long as the grid supports the field from the source, the grid could be interpolated to intervening points, but this would be inaccurate for coarse measurement grids.) The best focal length to use is not obvious, but half the ship length is often a good initial estimate, indicating a source length equal to the length of the ship. The main axis is chosen parallel to the centre line of the vessel.

D. Normalization of the harmonics & truncation of the SVD

The pseudoinverse of \mathbf{F} in Eq. (3) will be constructed using a singular value decomposition (SVD) following the Matlab function PINV. In this process, the basis functions are linearly combined such that the first new function holds the linear combination of the original set with the highest norm, the second one holds the linear combination from the remaining portion of the basis functions with highest norm etc.

Even small errors in the field (originating from noise, inaccuracies in the measurement arrangement or an early terminated basis set) may totally contaminate the estimated coefficients due to the ill-condition of the matrix \mathbf{F} . Truncating the pseudoinverse by only keeping basis functions that correspond to significant singular values, will reduce this sensitivity at the cost of larger truncation errors [3].

1) Normalization of the harmonics

The basis functions in the matrix \mathbf{F} have widely different scalings and therefore do not form an orthonormal set. Thus, the truncation of SVD of \mathbf{F} , may censor out one or several important harmonics so that the estimated coefficients are totally contaminated. This can only be remedied by scaling the harmonics so that their values reflect their relative importance compared to each other. Therefore, normalizing to the same maximum level on the measurement plane will be a good approach. Because an unfortunate choice of grid could lead to scaling of values near zero-points, we will instead use the energy outside the surface ellipsoid, $\xi = \xi_0$, given in [8]. The

basis functions in \mathbf{F} are properly normalized with $\sqrt{w_n^m}$:

$$w_n^m(\xi_0) = -\mu_0 \frac{\pi(1 + \delta(m, 0))(n+m)!}{2n+1(n-m)!} \cdot (\xi_0^2 - 1) Q_n^m(\xi_0) \cdot \frac{\partial}{\partial \xi_0} Q_n^m(\xi_0) \quad (6)$$

where δ is the Kronecker delta. We choose the coordinate ξ_0 such that the ellipsoid is tangent to the measurement grid, and find that the difference between the two normalizations is minimal.

Using this normalization, the higher degree and order harmonics are scaled down by a magnitude of roughly 6 for $n-m=8$, and up or down by as much as 10 magnitudes for higher indexed harmonics. Clearly this will have an influence on the result of truncation.

2) Truncation of the SVD

In order to choose a good threshold, first recall that the singular values are the weight of the linearly combined basis functions over the measurement grid. After the normalization, basis functions with significantly different range dependencies are all scaled to the same maximum level. Large singular values will therefore be determined by the samples near this maximum level. The smallest singular values must represent the remaining differences several magnitudes weaker.

For the following argument, assume that the functions were not scaled to unity at their largest value, but to the maximum measured field strength. Then identify the strongest field strength of the noise level and the minimum signature level at the border of the measurement grid. A basis function having this field strength throughout the measurement grid is not of much importance. We therefore choose the norm of this function as threshold for truncating the SVD.

IV. MEASURE OF QUALITY

In order to report the effect of each inversion criterion outlined in section III, a measure of quality is required. The quality measure is important in assessing the validity of the estimated model as is shown in section V and VI.

We choose to focus on two types of measures; one describing the near field, and one describing the far field.

A. Near field quality measure

For near field quality measure, we look at the relative error of the magnetic field at the plane of measurement. The average error on the grid points and in between the grid points will be used to generate two separate measures. Any difference in the two will indicate aliasing problems.

For the simulated sources, it is obvious to compare the field from the estimated model with the original source model. For

measured sources, we do not have the same possibility for evaluation between the original measurement points. However, for a reasonable dense sampling grid, interpolating between the points of measurement can be used as a first order approximation that allows for detecting at least severe aliasing problems.

B. Far field quality measure

For far field quality measure we choose the relative error on the (far field) magnetic dipole moment. From spherical harmonic series expansion we know that the lowest degree moment will be unchanged upon a displacement of the centre point [7]. For a prolate spheroidal series expansion, the same relation applies to the corresponding moment for any change of centre point or focal length. No magnetic monopoles exist, so the relation applies for the dipole moment.

The magnetic dipole moment $\mathbf{M} = [M_x, M_y, M_z]$ can be determined directly from the estimated expansion coefficients and the focal length using the relation of [6], to give

$$\mathbf{M} = \frac{4\pi f^2}{3} [c_1^0, 2c_1^1, 2s_1^1] \quad (7)$$

where c_1^0 , c_1^1 and s_1^1 are the non-normalized expansion coefficients.

Far field measurements can be used to determine the reference moment. If not available, the accuracy of the far field representation can be indicated by verifying that the dipole moment is conserved upon a change of centre point.

V. EVALUATION OF CRITICAL FEATURES

In this section a simulation study is done to quantify how the critical features outlined in section III are affecting the inverse problem of estimating the characteristics of a magnetic source from a limited number of measurements. In order to relate more closely to measuring the magnetic field of an unknown ship, we adopt the slightly erroneous centre point and focal length of the simulated source in the estimation. The actual source used will have a length of 72 m and the centre point at $[x, y, z] = [-7, 2, 1]$, but it is assumed to have a length of 78 m, and centred at the origin. Using the slightly erroneous centre point and focal length will in effect complicate the estimation as higher degree terms are introduced. The main axis of the source is known and the dipole moment used is $\mathbf{M} = [50, -20, 80] kAm^2$. All of these values are summarized in Table I.

TABLE I
TRUE AND APPROXIMATE CENTRE POINT AND FOCAL LENGTH

	True source	Approximation used
Centre point [m]	$[x, y, z] = [-7, 2, 1]$	$[x, y, z] = [0, 0, 0]$
Focal length [m]	$f = 36$	$f = 39$
Dipole moment	$\mathbf{M} = [50, -20, 80]kAm^2$	

True simulated source and approximation used during the estimation in order to relate to an unknown measured ship

A. Sampling criterion

The sampling criterion applies to the measurement grid used on a given source. The measurement plane is here chosen at a depth of $z=10$ m, and the x - and y -coordinates of the grid are outlined in Table II. The letters L, M and S will denote the large, medium and small grid, respectively.

TABLE II
MEASUREMENT GRIDS

Name	y-coordinate	x-coordinate.
Large	[-21:3:9]	[-60:1.2:60]
Medium	[-18:9:9]	[-60:1.2:60]
Small	[-9:18:9]	[-60:9.6:60]

The large, medium and small measurement grids, indicated by the start coordinate, the inter sample spacing and the stop coordinate

Fig. 1 shows the simulated source on each grid. All plotted fields are smooth in the along ship direction, but only the large grid give a good impression of the athwart ship dependency of the field. The medium grid does indicate the athwart ship dependency, but the corresponding information from the small grid is minimal. Therefore, the small grid can generally not be recommended for solving the inverse problem. However, for our simulated source of pure dipole moments, it will turn out to be applicable.

B. Supported harmonics

The harmonics of highest degree and order that can be distinguished on each of the three sampling grids of Table II are found from Eqs. (4) and (5) and are outlined in Table III.

TABLE III
MAXIMUM SUPPORTED SETS OF HARMONICS

Name	m_{\max}	ν_{\max}
Large	11	64
Medium	4	64
Small	2	7

Basis functions supported by each of the three sampling grids of Table II. The maximum supported degree n_{\max} for a given order m is found from the relation $n_{\max}(m) = \nu_{\max} + m$, following section III.B.

The effect of using various combinations of basis functions and measurement grids is tested. The results of the estimations are summarized in Table IV where the estimated relative errors are found from the total magnetic field, i.e., $|B_{\text{tot,est}} - B_{\text{tot}}|/B_{\text{tot}}$, averaged over all the measurements.

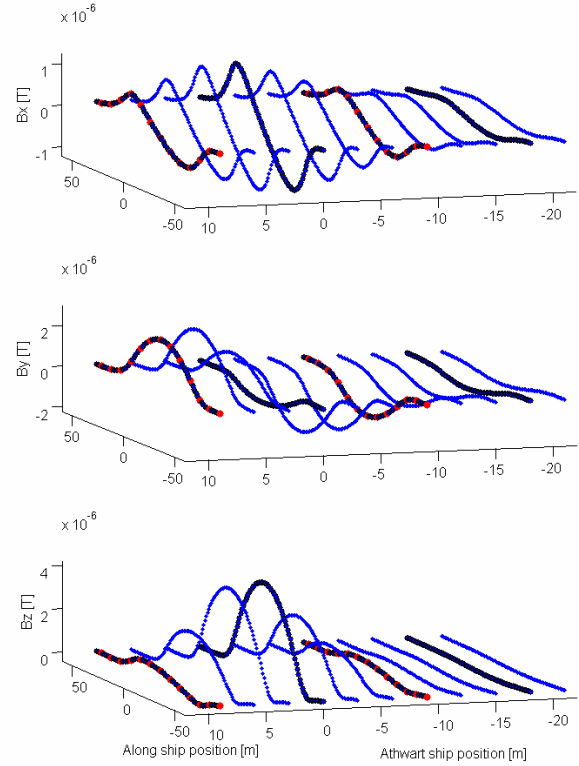


Fig. 1. The x -, y - and z -component of the simulated magnetic flux density in the top, centre and bottom window, respectively, simulated at a depth of 10 m. Red samples correspond to the small grid (S), the black samples correspond to the medium grid (M), and the blue samples correspond to the large grid (L).

TABLE IV

INVERSION BASED ON THE APPROXIMATE CENTRE POINT AND FOCAL LENGTH			
Meas. grid	L	M	S
Basis set	L	M	S
Dipole error	0.071	0.44	8.7
On-grid error	0.0048	0.047	2.7
Off-grid error	0.0047	0.048	2.8

Meas. grid	L	L	M	S
Basis set	M	S	L	L
Dipole error	0.69	12	0.050	9.3
On-grid error	0.10	7.2	0.0055	0.0030
Off-grid error	0.10	7.2	0.0055	17

All magnetic field errors are given in % and found from $|B_{\text{tot,est}} - B_{\text{tot}}|/B_{\text{tot}}$ averaged over all the measurements.

A dense sampling grid used along with the supported set of basis functions and our suggested normalization and threshold of truncation, gives a very good accuracy of the representation, despite the non-optimal choice of centre point and focal length.

When using the maximum supported basis sets, the on-grid error is of the same order of magnitude as the off-grid error, indicating no aliasing problems. Table IV also shows that the accuracy on describing both near field and far field increases with the size of grid and size of basis set.

Furthermore, the accuracy of the estimation is not significantly changed by introducing more sample points alone (in the absence of noise) if the basis set used is smaller than the maximum supported basis set for the grid stated in Table III.

By expanding the basis set out of the maximum supported set, the accuracy on the far field (expressed by the low degree coefficients) is increased. However, aliasing may be introduced (depending on the change of basis and truncation), leading to errors in the representation of the near field.

C. Choice of centre point and focal length

The conservation of the dipole moment has already been verified by inverting on a coordinate system with the focal length and the centre point different from those of the source. Here we will simply invert on the true centre point and focal length, and investigate the changed dependency on sampling grid and basis set. The results of the estimations are summarized in Table V. Comparing Table IV with Table V shows that the error is severely reduced or initially small for all the grids and basis sets.

TABLE V
INVERSION BASED ON THE TRUE CENTRE POINT AND FOCAL LENGTH

Meas. grid	L	M	S
Basis set	L	M	S
Dipole error	0.062	0.0044	0.00039
On-grid error	0.0012	0.0018	0.000077
Off-grid error	0.0012	0.0018	0.00010

Meas. grid	L	L	M	S
Basis set	M	S	L	L
Dipole error	0.013	0.19	0.044	3.9
On-grid error	0.0019	0.12	0.0014	0.0028
Off-grid error	0.0019	0.11	0.0014	9.2

All magnetic field errors are given in % and found from $|B_{tot_{est}} - B_{tot}|/B_{tot}$ averaged over all the measurements.

D. Normalization of the harmonics & truncation of the SVD

In this section we demonstrate the importance of the normalization of the harmonics and the truncation of the singular value decomposition for estimation of the expansion coefficients.

1) Truncation of the SVD

The effect of truncating in the singular value decomposition is found by repeating the estimation of the expansion coefficients with the truncation threshold set to zero. The results of the estimations are presented in Table VI.

TABLE VI
INVERSION WITHOUT TRUNCATION

Meas. grid	L	M	S
Basis set	L	M	S
Dipole error	0.98	0.46	8.7
On grid error	0.13	0.035	2.7
Off grid error	0.13	0.056	2.8

Meas. grid	L	L	M	S
Basis set	M	S	L	L
Dipole error	0.67	12	92 (63)	9.3
On grid error	0.099	7.2	21 (.002)	1e-12
Off grid error	0.10	7.2	21 (0.64)	16

All magnetic field errors are given in % and found from $|B_{tot_{est}} - B_{tot}|/B_{tot}$ averaged over all the measurements. (Matlab standard truncation gives close to exactly the same results. The only significant differences are given in parentheses.)

Most of the combinations of grid and basis set are similar to those with truncation applied, presented in Table IV. For the large grid with the supported basis set, the accuracy decreased by one order, but is still high. For the medium grid with an unsupported large basis set, the new result is way off.

We conclude that truncating the SVD of the normalized basis functions sometimes improves the accuracy significantly, and therefore should always be applied.

2) Normalization of the harmonics

The normalization of section V has been used for all the previous estimates of the expansion coefficients. In this section we investigate the importance of this normalization. The results of the estimation without normalization follow in Table VII.

TABLE VII
NON-NORMALIZED BASIS FUNCTIONS

Meas. grid	L	M	S
Basis set	L	M	S
Dipole error	670	1.4	10
On grid error	190	1.8	9.4
Off grid error	190	1.8	9.9

Meas. grid	L	L	M	S
Basis set	M	S	L	L
Dipole error	1.9	54	2e15	3e28
On grid error	2.9	27	120	17
Off grid error	2.9	27	120	140

All magnetic field errors are given in % and found from $|B_{tot_{est}} - B_{tot}|/B_{tot}$ averaged over all the measurements.

Table VII shows that a severe error may be introduced when using non-normalized harmonics as basis set. The results based on the true centre point are of the same order, and are therefore not tabulated. The corresponding estimation without truncation shows similar results for all combinations involving the largest basis set, while the other combinations are identical to the normalized (non-truncated) ones of Table VI. Therefore normalization of the harmonics is very important when estimating a PSH model of high degree or order, which is required for accurate representation of the field.

VI. MEASURED FIELD DATA OF A SHIP

In the following the gained insight from the previous sections is applied on the recorded static magnetic field data from a merchant ship. The ship is 78 m long and was measured at a Royal Norwegian Navy calibrations site. The vertical component of the magnetic field was measured on 11 sensors at 10 m water depth. A reference sensor a few hundred meters away was used for background field noise cancellation. The measurements were down-sampled to give roughly 0.6 m resolution in the along ship direction in the range of $[-60,+60]$ m, while athwart ship samples were between 21 m to port and 9 m to starboard side. The signatures are plotted in Fig. 2 with origin at the estimated centre of the vessel. The field strength in Fig. 2 has been scaled by an arbitrary scalar value.

We will now represent the field of this ship using a series expansion on prolate spheroidal harmonics by solving the inverse problem, following the approach outlined throughout this paper. From section III, we find that the grid supports discrimination between basis functions up to order $m = 5$ and degree expressed by $n - m = 64$.

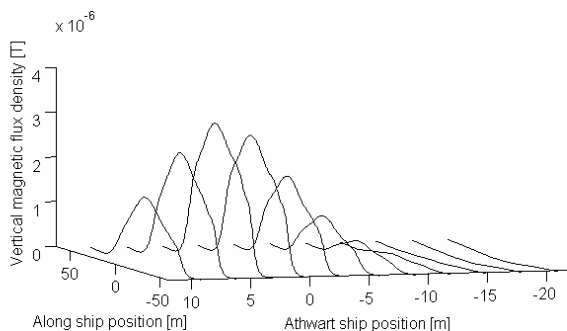


Fig. 2. The eleven signatures recorded for the merchant vessel of length 78 m. The field strength has been scaled by an arbitrary scalar value

Since the actual source of the ship is not known, it is important to assess the quality of the estimated model. We advocate that the methods suggested in section IV are highly applicable for such purposes and should be adopted as a standard for such validations.

We know that the dipole moments should be independent of the centre point and focal length, and therefore perform the inversion for several choices of coordinate systems. (The centre points and focal lengths are selected around the best assessment for the ship, so that the shifted source can be represented by the supported harmonics.) Furthermore, we evaluate the error of the field on the grid, and interpolate the measured field to give a rough estimate of the error off the grid. Together this should give enough information to validate the process of inversion and the generated model.

The estimation results for the various centre points and focal lengths are presented in Table VIII. We find that the error on the grid is very small, and also the error off the grid is small considering that the reference field was found by interpolation

between the measurement points. The dipole moments are not very stable, and are estimated to $\mathbf{M} = [-12.5 \pm 8.3, -32.5 \pm 5.3, 115 \pm 10]$ with one standard deviation indicated. The large variance indicates that the far field is not accurately represented by the estimated expansion coefficients.

The shortcoming of the far field representation could either originate from inaccuracies on solving the inverse problem, or from insufficient information in the employed set of magnetic measurements.

To summarize, the obtained model of this ship accurately represents the field near the measurement plane, but for larger distances the accuracy is gradually lost.

TABLE VIII
REPRESENTATIONS OF THE MEASURED MAGNETIC FIELD OF THE SHIP

Centre point [m] f	x,y,z	Estimated dipole moment \mathbf{M} [kAm^2]	Estimated field error	
			On-grid	Off-grid
39	0, 0, 0	-12.8, -33.4, 114	0.032	0.24
35	0, 0, 0	-11.7, -34.2, 112	0.038	0.24
43	0, 0, 0	-10.1, -32.6, 115	0.029	0.21
39	4, 0, 0	-25.6, -32.6, 115	0.031	0.22
39	-4, 0, 0	3.3, -34.7, 112	0.035	0.30
39	0, 2, 0	-19.6, -39.7, 101	0.032	0.32
39	0, -2, 0	-5.8, -20.1, 132	0.036	0.22
39	0, 0, 2	-18.0, -30.4, 102	0.033	1.7
39	0, 0, -2	-12.5, -34.6, 129	0.032	0.18

Dipole moments estimated from measured vertical magnetic field from the merchant ship of length 78 m. The focal lengths are selected around the half the value of the ship length, and the centre point around an approximated geometric centre. The estimated field error is found from $|\mathbf{B}_{z\text{-est}} - \mathbf{B}_z| / |\mathbf{B}_z|_{\text{max}} \cdot 100\%$, averaged over all the measurements. The off-grid reference is found by cubic interpolation between the measurement points.

VII. CONCLUSION

A number of improvements have been demonstrated for the inverse problem of prolate spheroidal harmonics series expansion. Limiting the set of harmonics to those supported by the measurement grid, normalizing and utilizing truncated singular value decomposition, contributes to a major combined effect. The resulting series expansion describes the near field very accurately and without aliasing. Given sufficient information from near field measurements, even the far field can be accurately represented. A set of quality measures is suggested and used to validate the application of the method on real measurements. The findings using real measurement are in accordance with those of simulated sources.

REFERENCES

- [1] A. V. Kildishev et al, "Zonal magnetic signatures in spherical and prolate spheroidal analysis", Proc. Marelec, 1999.
- [2] M. Brisan et al, "Using global optimisation techniques to solve the inverse problem for the computation of the static magnetic signature of ships, Proc. Marelec, 2001.
- [3] R. Kamondetdacha and A. V. Kildishev, "Multipole characterization of a magnetic source using truncated SVD", IEEE Trans. Magn. vol 40, pp. 2176-2178, 2004.
- [4] M. Abramowitz and I. A. Stegun (editors), "Handbook of mathematical functions", 10th printing, US National Bureau of Standards, 1972.
- [5] A. Gil and J. Segura, "A code to evaluate prolate and oblate spheroidal harmonics", Comput. Phys. Commun., vol. 108, pp 267-278, 1998.
- [6] D. A. Nixon and F. E. Baker, "Using prolate spheroidal distributions for magnetic modeling", J. Appl. Phys. 52, pp. 539-541, 1981.
- [7] J. D. Jackson, "Classical electrodynamics", 3rd ed. Chapter 4.1, John Wiley & Sons Inc, New York.
- [8] A. V. Kildishev and J. A. Nyenhuis, "External magnetic characterization of marine vehicles", Oceans 2000 MTS/IEEE Conference and Exhibition, pp 1145-1147, 2000.